Supporting information for

Development of a Novel Core-Shell-Magnetic Fe_3O_4@CMC@ZIF-8-OH Composite with Outstanding Rubidium Ion Capacity

Ning Tian,† Jiafei Wu,† Jiaqi Wang,†and Wei Dai*,†

†College of Chemistry and Life Science, Zhejiang Normal University, Zhejiang Province Jinhua 321004, People's Republic of China

Corresponding Author

Prof. Wei Dai

*E-mail: daiwei@zjnu.edu.cn. Phone: +86-579-82282269. Fax: +86-579-82282325.

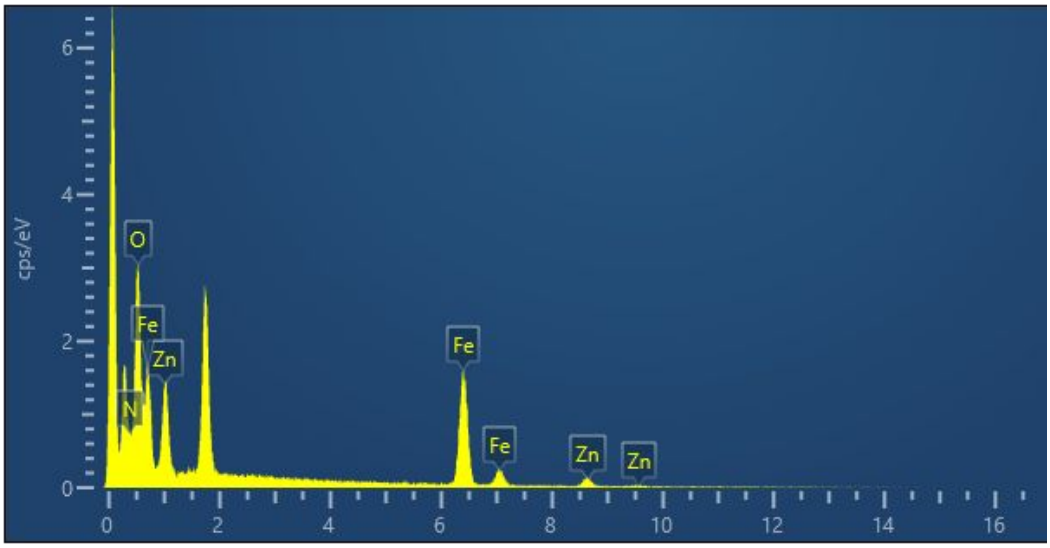

Figure S1. The EDX spectra of Fe_3O_4@CMC-12@ZIF-8 sample.

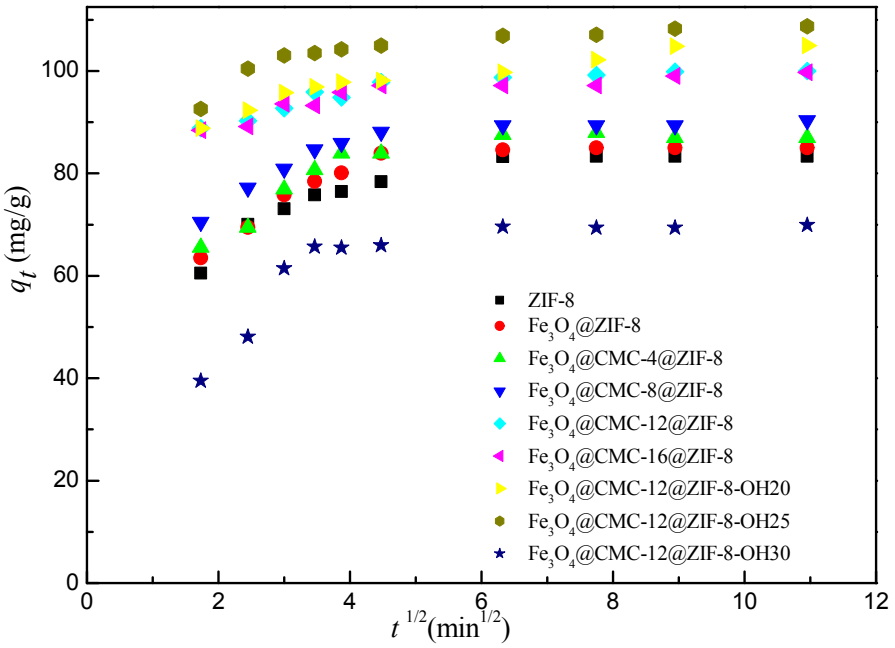

Figure S2. Weber–Morris intra-particle diffusion plots for the adsorption of Rb^+ on as-prepared adsorbents in this work.

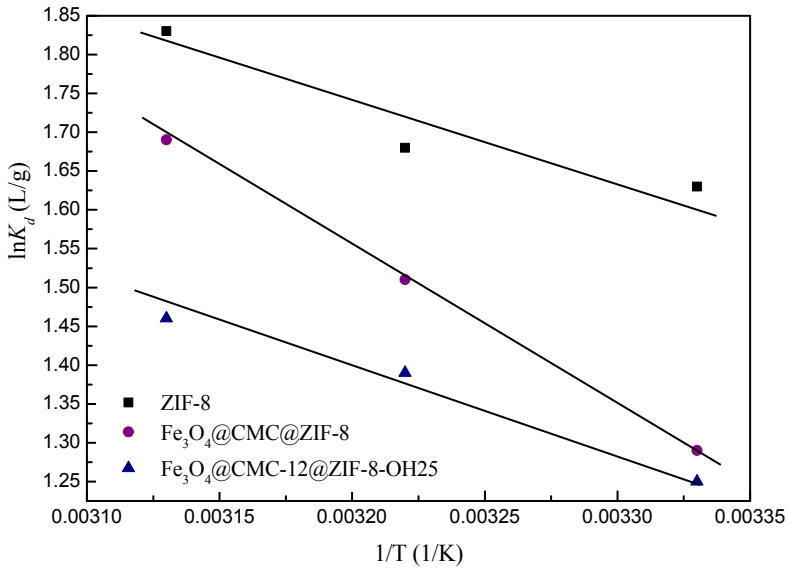

Figure S3. Plots of lnK_d versus 1/T for ZIF-8, Fe_3O_4@CMC@ZIF-8, and Fe_3O_4@CMC-12@ZIF-8-OH25, respectively.

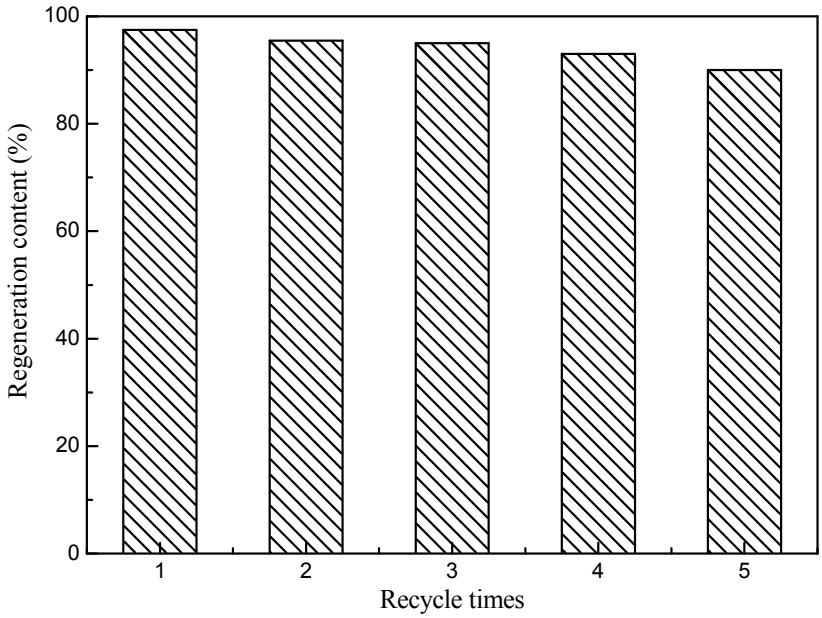

Figure S4. Effect of recycle times of Fe_3O_4@CMC-12@ZIF-8OH25 on the Rb^+ adsorption capacity.

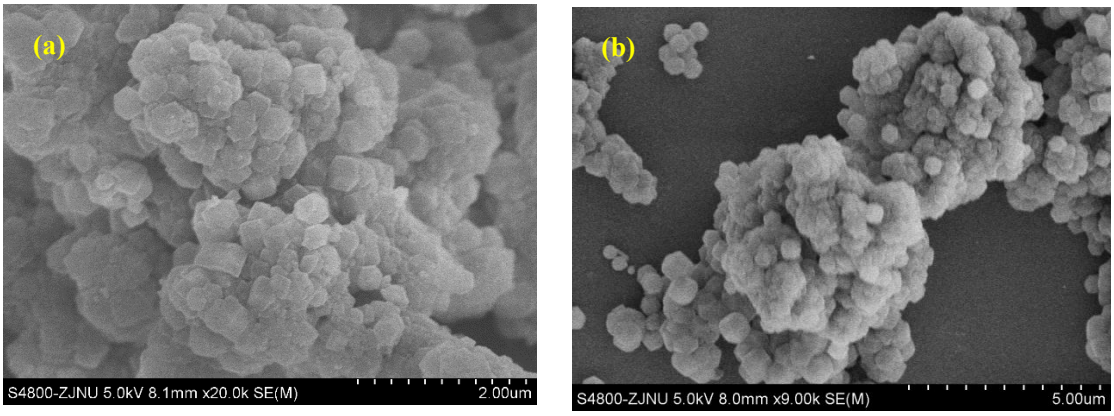

Figure S5. The SEM images of Fe_3O_4@CMC-12@ZIF-8-OH25 samples before and after Rb^+ adsorption from water. (a): before adsorption; (b): after adsorption.

Table S1. Maximum adsorption capacities of Rb^+ on various adsorbents.

Adsorbents	Adsorption conditions	Maximum adsorption capacity ($mg \cdot g^{-1}$)	Reference
Ion-imprinted polymer	pH: 9.0;25℃	5	[1]
CA/$Na_2Ti_3O_7$	pH: 5.5;25℃	95	[2]
Potassium cobalt hexacyanoferrate	pH: 7.0 ± 0.5;25℃	96	[3]
$K_3[Fe(CN)_6]$	pH: 7.8; 21℃	47	[4]
$K_3[Fe(CN)_6]$/PMMA	pH: 7.0; 25℃	80	[5]
AMoP-Calcium alginate	pH: 3.5; 25℃	50	[6]
ZrP	pH: 3.0; 25℃	61	[7]
PMoZr	pH: 3.0; 25℃	63	[7]
IMOMTZ	pH: 4.0; 25℃	26	[8]
ZIF-8	pH: 7.0; 25℃	83	this work
Fe_3O_4@CMC12@ZIF-8	pH: 7.0; 25℃	100	this work
Fe_3O_4@CMC-12@ZIF-8-OH25	pH: 7.0; 25℃	109	this work

Table S2. Textural properties of ZIF-8, Fe_3O_4, Fe_3O_4@CMC-12@ZIF-8 and Fe_3O_4@CMC-12@ZIF-8OH25.

Sample	S_{BET} (m^2/g)	V_{total} (cm^3/g)	V_{meso} (cm^3/g)	V_{mic} (cm^3/g, %)	Average pore diameter (nm)
ZIF-8	1636	0.66	0.05	0.61, 92%	1.24
Fe_3O_4	16	0.011	0.106	0.004, 36%	0.005
Fe_3O_4@CMC-12@ZIF-8	1124	0.47	0.06	0.41, 87%	1.22
Fe_3O_4@CMC-12@ZIF-8OH25	919	0.36	0.05	0.31, 86%	1.07

Table S3. Elemental compositions of Fe_3O_4@CMC-12@ZIF-8 sample according to EDX analysis

Element	Weight percent, wt%	Atomic molar percent, %
C	21.88	35.53
O	24.01	29.27
Fe	27.59	9.63
Zn	10.37	3.09
N	16.15	22.48
Total	100	100

Table S4. Isotherm models used in this study and their linear forms.

Isotherm	Nonlinear form	Linear form	Plot	Eqs.
Langmuir	$q_e = \frac{K_L C_e}{1 + K_L C_e}$	$\frac{C_e}{q_e} = \frac{1}{q_L \cdot K_L} + (\frac{1}{q_L}) \cdot C_e$	$\frac{C_e}{q_e}$ versus C_e	(2)
Freundlich	$q_e = K_f C_e^{\frac{1}{n}}$	$\ln q_e = \ln K_f + (\frac{1}{n}) \cdot \ln C_e$	$\ln q_e$ versus $\ln C_e$	(3)
Temkin	$e^{qe} = (K_T C_e) \frac{RT}{b_T}$	$q_e = \frac{RT}{b_T} \ln K_T + \frac{RT}{b_T} \ln C_e$	q_e versus $\ln C_e$	
D-R	$q_e = q_s e^{(-K_D \varepsilon^2)}$	$\ln q_e = \ln q_s - K_D \varepsilon^2$	$\ln q_e$ versus ε^2	(4)

Where q_e is the maximum capacity of adsorption in mg/g; K_L and K_T is a constant related to the affinity of the binding sites in L/mg; 'K_f' and 'n' are the measures of adsorption capacity and intensity of adsorption; R is the universal gas constant; b_T is related to the heat of adsorption in kJ/mol.

Table S5. Constants and correlation coefficients of different adsorption models

Samples	Langmuir			Freundlich			Temkin			D-R		
	q_m (mg/g)	K_L (L/mg)	R^2	K_f (L/g)	n	R^2	b_T (kJ/mol)	K_T (L/g)	R^2	q_s (mg/g)	K_D (mol^2/kJ^2)	R^2
ZIF-8	75.7	0.0151	0.24	1.2708	1.0310	0.99	79.8006	0.1305	0.91	52.78	0.000018	0.71
Fe_3O_4@CMC@ZIF-8	81.8	0.0984	0.84	0.8461	0.8971	0.99	70.8004	0.1229	0.92	58.50	0.000022	0.78
Fe_3O_4@CMC-4@ZIF-8	85.7	0.0052	0.59	1.5005	1.0189	0.99	71.5926	0.1433	0.91	58.39	0.000015	0.66
Fe_3O_4@CMC-8@ZIF-8	90.6	0.0090	0.88	1.6832	1.0206	0.99	67.7004	0.1497	0.92	62.13	0.000013	0.68
Fe_3O_4@CMC-12@ZIF-8	96.3	0.0167	0.86	2.8732	1.1499	0.99	68.1241	0.1805	0.92	66.09	0.000093	0.64
Fe_3O_4@CMC-16@ZIF-8	92.7	0.0070	0.70	1.2915	0.9379	0.99	67.4652	0.1582	0.92	62.16	0.000011	0.70
Fe_3O_4@CMC-12@ZIF-8OH20	104.1	0.0079	0.86	3.0027	1.1256	0.99	60.5719	0.1739	0.93	78.12	0.000014	0.83
Fe_3O_4@CMC-12@ZIF-8OH25	109.1	0.0105	0.82	3.1750	1.0939	0.99	58.1312	0.1976	0.92	83.69	0.000011	0.80
Fe_3O_4@CMC-12@ZIF-8OH30	71.2	0.0061	0.72	0.4086	0.8095	0.99	70.2400	0.0875	0.95	54.86	0.000047	0.80

References

(1) Dai, W.; Fang, Y. Y.; Yu, L.; Zhao, G. H.; Yan, X. Y. Rubidium ion capture with composite adsorbent PMA@HKUST-1. *J. Tanwan. Inst. Chem. E.* **2018**, *84*, 222–228.

(2) Yu, L.; Liu, Q.; Dai, W.; Tian, N.; Ma, N. Efficient thiophene capture with a hydrophobic Cu-BTC-(n)Br adsorbent in the presence of moisture. *Micropor. Mesopor. Mat.* **2018**, *266*, 7–13.

(3) Wei Dai, Yaoyao Fang, Le Yu, Guihua Zhao, Xiaoying Yan, Rubidium ion capture with composite adsorbent PMA@HKUST-1. *J. Tanwan. Inst. Chem. E.* **2018**, *84*, 222–228.

(4) Li, T.; Zhang, W.; Zhai, S.; Gao, G.; Ding, J.; Zhang W.; Liu, Y.; Zhao, X.; Pan, B.; Lv, L. Effificient removal of nickel(II) from high salinity wastewater by a novel PAA/ZIF-8/PVDF hybrid ultrafifiltration membrane. *Water Research* **2018**, *143*, 87–98.

(5) Park, K. S.; Ni, Z.; Côté, A. P.; Choi, J. Y.; Huang, R.; Uribe-Romo, F. J.; Chae, H. K.; O'Keeffe, M.; Yaghi, O. M. *Proc. Natl. Acad. Sci.* U.S.A., **2006**, *103*, 10186–10191.

(6) Hashemi, B.; Shamsipur, M.; Synthesis of novel ion-imprinted polymeric nanoparticles based on dibenzo-21-crown-7 for the selective pre-concentration and recognition of rubidium ions, *J. Sep. Sci.* **2015**, *38*, 4248–4254.

(7) Liu, G.; Mei, H. Y.; Tan, X. L.; Zhang, H. F.; Liu, H. N.; Fang, M.; Wang, X. K.; Enhancement of Rb^+ and Cs^+ removal in 3D carbon aerogel-supported $Na_2Ti_3O_7$, *J. Mol. Liq.* **2018**, *262*, 476–483.

(8) Naidu, G.; Nur, T.; Loganathan, P.; Kandasamy, J.; Vigneswaran, S. Selective sorption of rubidium by potassium cobalt hexacyanoferrate, *Sep. Purif. Technol.* **2016**, *163*, 238–246.

Table S6. Calculation equations.

Name	Equations
Pseudo-first order model	$\ln(q_e - q_t) = \ln(q_e) - K_1 t$
Pseudo-second order model	$\frac{t}{q_t} = \frac{1}{K_2 q_e} + \frac{t}{q_e}$
Intra-particle diffusion model	$q_t = K_3 t^{1/2}$

Where q_e and q_t (mg/g) are the uptakes of thiophene at equilibrium and at time t (min), respectively, K_1 (1/min) is the adsorption rate constant, K_2 (g/mg.min) is the rate constant for the second-order equation, and K_3 (mg/g.min$^{1/2}$) is the intra-particle diffusion rate constant.

Where $q_{e,exp}$ and $q_{e,cal}$ are the experimental and calculation uptakes of adsorbates, respectively.

Table S7. Kinetic parameters for Rb^+ adsorption on ZIF-8, Fe_3O_4@CMC@ZIF-8 and Fe_3O_4@CMC@ZIF-8OH, respectively.

Samples	Pseudo-first-order rate equation						Pseudo-second-order rate equation					Intra-particle diffusion model		
	$q_{e,exp}$ (mg/g)	$q_{e,cal}$ (mg/g)	K_1 (1/min)	R^2	$\triangle q$ (mg/g)	$\triangle q$ (%)	$q_{e,cal}$ (mg/g)	K_2 (g/mg·min)	R^2	$\triangle q$ (mg/g)	$\triangle q$ (%)	C (mg/g)	K_3 (mg/g·min$^{1/2}$)	R^2
ZIF-8	84	11.91	-0.0586	0.776	72.09	85.82	84.53	0.0094	0.999	-0.53	-0.63	66.09	2.0141	0.651
Fe_3O_4@CMC@ZIF-8	85	7.00	-0.0413	0.404	78.31	92.12	85.25	0.0141	0.999	-0.25	-0.29	69.21	1.8451	0.532
Fe_3O_4@CMC-4@ZIF-8	87	8.08	-0.0323	0.325	78.92	90.72	88.11	0.0116	0.999	-1.11	-1.27	70.27	2.0230	0.564
Fe_3O_4@CMC-8@ZIF-8	94	18.86	-0.0369	0.787	75.14	79.94	93.02	0.0075	0.999	0.98	1.04	74.96	1.8706	0.662
Fe_3O_4@CMC-12@ZIF-8	100	10.11	-0.0496	0.975	89.89	89.89	100.50	0.0153	0.999	-0.50	-0.50	89.76	1.1449	0.720
Fe_3O_4@CMC-16@ZIF-8	99	11.04	-0.0399	0.879	87.96	88.84	99.90	0.0130	0.999	-0.90	-0.90	89.24	1.0961	0.711
Fe_3O_4@CMC-12@ZIF-8-OH20	105	13.67	-0.0374	0.639	91.33	86.99	105.15	0.0086	0.999	-0.15	-0.14	90.00	1.5291	0.840
Fe_3O_4@CMC-12@ZIF-8-OH25	109	11.18	-0.0426	0.944	97.82	89.74	109.17	0.0135	0.999	-0.17	-0.15	97.36	1.2499	0.670
Fe_3O_4@CMC-12@ZIF-8-OH30	70	5.58	-0.0410	0.202	64.44	90.06	70.52	0.0094	0.999	-0.52	-0.75	49.84	2.3664	0.430

Table S8. Thermodynamics adsorption parameters for Rb^+ on adsorbents.

Adsorbents	T (°C)	K_d	ΔG	ΔH	ΔS
ZIF-8	25	4.75	-3.88	40.61	8.26
	35	5.11	-4.15		
	45	6.08	-4.64		
Fe_3O_4@CMC@ZIF-8	25	3.43	-3.09	65.22	16.85
	35	4.38	-3.75		
	45	5.37	-4.41		
Fe_3O_4@CMC-12@ZIF-8-OH25	25	3.65	-3.19	29.25	5.66
	35	3.74	-3.35		
	45	4.28	-3.79		